J Solid State Electrochem (2012) 16:731–738
DOI 10.1007/s10008-011-1418-4

ORIGINAL PAPER

Determination aminopyrine in pharmaceutical formulations based on APTS-Fe_3O_4 nanoparticles modified glassy carbon electrode

Huanshun Yin · Yunlei Zhou · Tao Liu · Tiantian Tang · Shiyun Ai · Lusheng Zhu

Received: 11 December 2010 / Revised: 24 April 2011 / Accepted: 25 April 2011 / Published online: 12 May 2011

Abstract In this work, 3-aminopropyltriethoxysilane modified Fe_3O_4 nanoparticles (ATPS-Fe_3O_4) were used to modify glassy carbon electrode for aminopyrine determination. ATPS-Fe_3O_4 showed obviously catalytic activity and adsorptivity towards aminopyrine oxidation proven by the increased oxidation peak current and the decreased oxidation peak potential. The best analytical response was obtained by immobilizing 8 μL 3 mg/mL ATPS-Fe_3O_4 dispersion with an accumulation time of 200 s at −0.2 V in 0.1 M phosphate buffer solution (pH 9.0). The oxidation peak current of aminopyrine showed linear relationship with its concentration in the range from 0.5 to 100 and 100 to 1600 μM. The detection limit was 0.1 μM (S/N=3). The proposed method showed satisfactory repeatability and anti-interference ability. The fabricated electrode was successfully applied to determine aminopyrine in pharmaceutical formulations.

Keywords Aminopyrine · 3-Aminopropyltriethoxysilane · Fe_3O_4 magnetic nanoparticles · Electrochemical determination · Pharmaceutical formulations

H. Yin · T. Liu · S. Ai (✉)
College of Chemistry and Material Science,
Shandong Agricultural University,
Taian 271018 Shandong, China
e-mail: ashy@sdau.edu.cn

H. Yin · T. Tang · L. Zhu (✉)
College of Resources and Environment,
Shandong Agricultural University,
Taian 271018 Shandong, China
e-mail: lushzhu@sdau.edu.cn

Y. Zhou
College of Life Science, Beijing Normal University,
100875, Beijing, China

Introduction

Aminopyrine (4-dimethylamino-2,3-dimethyl-1-phenyl-3-pyrazolin-5-one, CAS No. 58-15-1) has been widely used as an analgesic and antipyretic drug. Because aminopyrine can cause agranulocytosis and bone marrow suppression, decrease the amount of white blood cell, and form nitrosamines which are carcinogenic substances, now it has been forbidden to use alone clinically. However, in China, aminopyrine is still used as one of the components of compound pharmaceuticals on treating febrile patients, such as aminopyrine and caffeine tablets, compound amantadine hydrochloride tablets, compound aminopyrine phenacetin and caffeine tablets, compound aminophenzone injection, and aminophenazoneco. There are many poisoning cases caused by overdose injection of aminopyrine and some caused by violation of operating practices and wrong route of administration by intravenous overdose [1]. Therefore, the determination of aminopyrine content in pharmaceuticals is necessary.

Up to now, several methods have been developed for the determination of aminopyrine, such as spectrophotometry [2], capillary electrophoresis-electrochemical detection (CE-ED) [3], liquid chromatography–tandem mass spectrometry (LC–MS–MS) [1], high-performance liquid chromatography (HPLC) [4], reverse-phase chromatography/amperometric detection (RPC–AD) [5] and high-performance liquid chromatography–electrochemistry (HPLC–ED) [6]. These methods require complicated sample pretreatment, large-size instrument, and skilled operator. Moreover, these methods are also time-consuming. Recently, purely electrochemical techniques have attracted more and more attentions on pharmaceuticals determination and monitoring [7–9]. Compared with other methods, purely electrochemical methods showed obvious advantages, such as fast response, cheap

instrument, low cost, simple operation, time saving, high sensitivity, excellent selectivity, and real-time detection in situ condition.

With the development of nanotechnology, more and more nanomaterials with good catalytic activity, adsorptivity, and electroconductivity have been synthesized and widely used as electrode modification materials, such as carbon nanotubes [10], graphene [11], gold nanoparticles [12], silver nanoparticles [13], TiO_2 [14], ZnO [15], CdS [16], Fe_3O_4 [17], Al_2O_3 [18], CoTe [19], hydroxyapatite [20, 21], and so on. Among them, magnetic Fe_3O_4 nanoparticles have aroused great interest due to their good biocompatibility, strong superparamagnetic property, low toxicity, and easy preparation [22, 23]. However, Fe_3O_4 nanoparticles in solution phase are easy to aggregate, which limits their application. For this reason, various functionalized Fe_3O_4 nanoparticles were investigated to improve the dispersion, for instances, Fe_3O_4@Pt core-shell nanoparticles [24], Fe_3O_4 Core/Au Shell nanoparticles [25], and Fe_3O_4@SiO_2 magnetic nano \particles [26]. It has been reported that the surface of Fe_3O_4 magnetic nanoparticles can also be functionalized with 3-aminopropyltriethoxysilane ($NH_2(CH_2)_3Si(OC_2H_5)_3$, APTS). These APTS-functionalized Fe_3O_4 nanoparticles (APTS-Fe_3O_4) could significantly improve the protein immobilization [27]. However, the application of APTS-Fe_3O_4 in electrochemical sensor has not yet been reported.

In this work, APTS-Fe_3O_4-modified glassy carbon electrode (APTS-Fe_3O_4-GCE) was fabricated and used to determine aminopyrine in pharmaceutical formulations. The electrochemical behavior of aminopyrine was investigated by cyclic voltammetry, chronocoulometry and differential pulse voltammetry. Some factors influencing the determination, such as APTS-Fe_3O_4 immobilization amount, pH, accumulation time, and accumulation potential, were optimized to obtain the optimal determination results. Because the electrode preparation process is simple and easy, the determination does not need costly and complicated instrument; the proposed method is sensitive and selective, and it is expected that APTS-Fe_3O_4-GCE can be applied to determine aminopyrine in practice.

Experimental

Reagents and apparatus

Aminopyrine and APTS were purchased from Aladdin (China). Aminopyrine and caffeine tablets (aminopyrine content, 0.15 g/tablet) were from Jilin Weikang Medicine Co., Ltd. (China). Compound amantadine hydrochloride tablets (aminopyrine content, 0.15 g/tablet) were from Jinlin Jinquan Baoshan Medicine Co., Ltd. (China). Compound aminopyrine phenacetin and caffeine tablets (aminopyrine content, 0.1 g/tablet) were from Shanxi Yuanjing Kangye Medicine Co., Ltd. (China). Compound aminophenzone injection (aminopyrine content, 0.0715 g/ml) was from Sichuan Weierkang Group (China). Compound aminopyrine and antipyrine injection (aminopyrine content, 0.05 g/mL) was from Shanxi Yinhu medicine Co., Ltd. (China). The stock solution of aminopyrine (0.1 M) was prepared with anhydrous ethanol and kept in darkness at 4 °C. Working solutions were freshly prepared before use by diluting the stock solution with anhydrous ethanol. 0.1 M phosphate-buffered saline (PBS) were prepared by mixing the stock solution of 0.1 M NaH_2PO_4 and 0.1 M Na_2HPO_4, and the pH was adjusted by NaOH or HCl. All chemicals were analytical reagent grade and used without further purification. All solutions were prepared with double distilled deionized water, which was prepared by distilling the deionized water using automatic dual distilled water device (model 1018-B, Jiangsu, China) made by quartz.

Electrochemical experiments were performed with CHI660C electrochemical workstation (Shanghai Chenhua Co., China) with a conventional three-electrode cell. A bare or APTS-Fe_3O_4 modified GCE (CHI104, d= 3 mm) was used as working electrode. A saturated calomel electrode (SCE) and a platinum wire were used as reference electrode and auxiliary electrode, respectively. The transmission electron microscope (TEM) image was obtained at JEOL-1200EX TEM (Japan). The image of scanning electron microscope (SEM) was obtained at JSM-6610LV (Japan). All the measurements were carried out at room temperature.

Preparation of APTS-Fe_3O_4

The APTS-Fe_3O_4 magnetite nanoparticles were synthesized according to previous report [27] with minor modification. Briefly, a mixed solution of $FeCl_3$ (0.2 M) and $FeSO_4$ (0.1 M) was prepared in double distilled deionized water. Then, ammonia aqueous solution (20%) was dropped into it with violently stirring until the pH of the solution raised to 10. After incubation for 30 min at 80 °C, the mixture was cooled to room temperature with stirring, and the resulting magnetic Fe_3O_4 nanoparticles were separated magnetically and washed by double distilled deionized water for five times to remove the excess ammonia and then formed suspension by ultrasonication. 1.5 g Fe_3O_4 suspension were added to a freshly prepared solution of APTS (2% v/v) in water and the final volume adjusted to 150 ml. The mixture was allowed to react with vigorous stirring on a magnetic stirrer for 7 h at 70 °C and washed five times with double distilled deionized water using a magnetic separator and then dried into powder at room temperature under vacuum.

Preparation of APTS-Fe_3O_4-GCE

Before modification, the bare GCE (3 mm in diameter) was polished to a mirror-like with 0.05 μm alumina slurry on micro-cloth pad and rinsed thoroughly with double distilled deionized water between each polishing step, then washed successively with double distilled deionized water, anhydrous alcohol, and double distilled deionized water in an ultrasonic bath and dried in air before use.

For preparation of APTS-Fe_3O_4-GCE, 3 mg/mL APTS-Fe_3O_4 dispersion was first prepared with double distilled deionized water, followed by ultrasonication for 2 h. With a microinjector, 8 μL of APTS-Fe_3O_4 dispersion was deposited on the freshly prepared GCE surface. After the solvent was evaporated under room temperature, the electrode surface was thoroughly rinsed with double distilled deionized water and dried under ambient condition. The modified electrode was stored at 4 °C in a refrigerator when not in use.

Electrochemical measurements

Electrochemical impedance measurements were carried out in 0.1 M KCl solution containing 5 mM $K_3[Fe(CN)_6]$/$K_4[Fe(CN)_6]$ (1:1, molar ratio). The electrochemical impedance spectra (EIS) were recorded in the frequency range of 10^5 to 10^{-1} Hz. Cyclic and differential pulse voltammetry measurements were carried out in unstirred 0.1 M PBS (pH 9.0) at room temperature, and all potentials were measured and reported vs. SCE. In a typical process, 10 mL of PBS was transferred to a clean, dry electrochemical cell, and the required volume of aminopyrine or sample solutions was added by microinjector. After accumulation for 200 s at −0.2 V, the cyclic voltammetry was performed from 0 to 0.7 V and the differential pulse voltammogram was recorded from 0 to 0.6 V.

Sample preparation

Ten tablets were selected at random, thoroughly pulverized in an agate mortar and mixed. An amount equivalent to a single tablet was dissolved in 30 mL anhydrous ethanol. After filtered with 0.45 μm polytetrafluoroethylene microfiltration membrane, the filtrate was collected in a 50-mL volumetric flask and diluted to the mark by anhydrous ethanol. The injection containing aminopyrine was used as received.

Results and discussion

Characterization of APTS-Fe_3O_4-GCE

Figure 1A was the TEM image of the magnetite nanoparticles coated with APTS, which showed that most of the particles are quasi-spherical with an average diameter of about 25 nm. The typical morphologies of GCE (B) and APTS-Fe_3O_4-GCE (C) were also shown in Fig. 1. It can be seen that the GCE surface was plain. When APTS-Fe_3O_4 was immobilized on the GCE surface, an irregular and

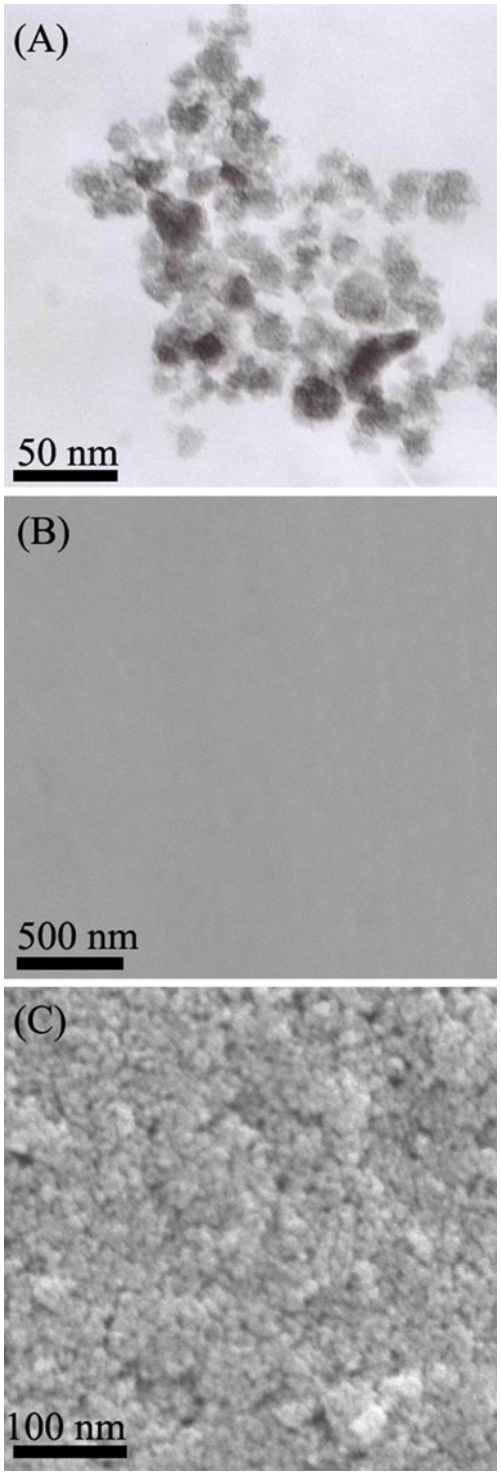

Fig. 1 TEM image of APTS-Fe_3O_4 (**A**), SEM images of GCE (**B**), and APTS-Fe_3O_4-GCE (**C**)

porous surface was observed. It is clear that the electrode surface can be increased according to the porous morphology of APTS-Fe_3O_4-GCE, which was further confirmed by chronocoulometry (see "Chronocoulometry").

EIS can give information on the impedance changes of the electrode surface. In EIS, the semicircle diameter equals to the electron transfer resistance (R_{et}). The changes of the value of R_{et} can reflect the electrode modification process. By using $K_3[Fe(CN)_6]/K_4[Fe(CN)_6]$ redox couple as an electrochemical probe, the Nyquist plots of different electrodes in the frequency range from 10^5 to 10^{-1} Hz were obtained (Fig. 2). The semicircle diameter of APTS-Fe_3O_4-GCE (curve b) in Nyquist plot was higher than that of the bare GCE (curve a), indicating that the electron transfer of the redox probe decreased in the presence of APTS-Fe_3O_4. This phenomenon can be attributed to APTS, which increases the electron transfer resistance and blocks the electron exchange between the redox probe and electrode surface. The increased electron transfer resistance also demonstrated that APTS-Fe_3O_4 was successfully immobilized on the GCE surface.

Electrochemical behavior of aminopyrine at APTS-Fe_3O_4-GCE

For proving the advantages of APTS-Fe_3O_4-GCE, the electrochemical behavior of aminopyrine was investigated in 0.1 M PBS by GCE and APTS-Fe_3O_4-GCE, respectively. As can be seen in Fig. 3, no redox peak was observed in the blank PBS for both electrodes; this indicates that APTS-Fe_3O_4 is electroinactive in the selected potential range. When aminopyrine was added into the PBS, a wide and weak oxidation peak was obtained at 0.49 V, which can be attributed to the oxidation of aminopyrine. In the reverse scan process, a very weak reduction peak was observed with the reduction

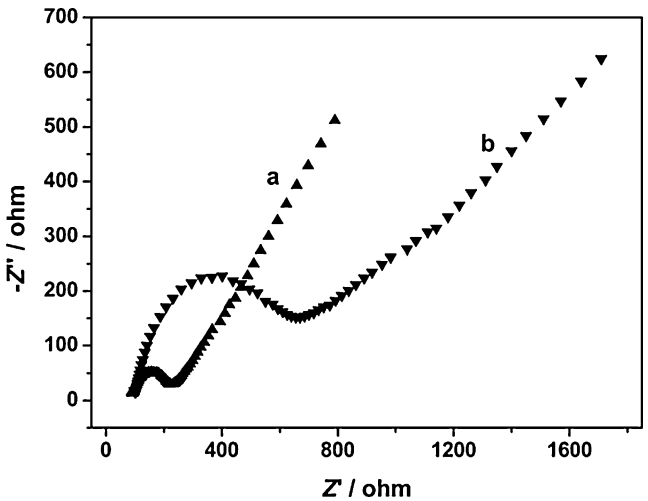

Fig. 2 Electrochemical impedance spectra for GCE (*a*) and APTS-Fe_3O_4-GCE (*b*) in 5 mM $[Fe(CN)_6]^{3-}/[Fe(CN)_6]^{4-}$ (1:1) solution containing 0.1 M KCl with the frequencies swept from 10^5 to 10^{-1} Hz

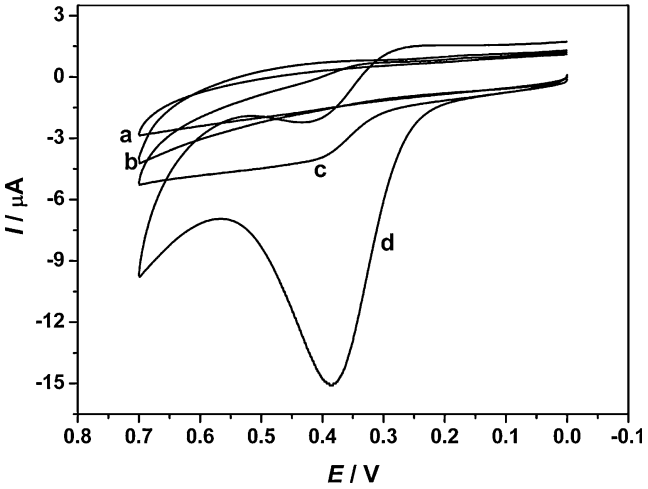

Fig. 3 Cyclic voltammograms of GCE (*a*, *c*) and APTS-Fe_3O_4-GCE (*b*, *d*) in the absence (*a*, *b*) and presence (*c*, *d*) of 0.2 mM aminopyrine in 0.1 M PBS (pH 9.0). Scan rate, 100 mV/s; accumulation time, 200 s; accumulation potential, −0.2 V

potential of 0.3 V, implying that the electrochemical behavior of aminopyrine is a quasi-reversible process. The peak-to-peak separation (ΔE_p) is 0.19 V, indicating a slow electron transfer rate. However, the redox peak currents of aminopyrine obtained at APTS-Fe_3O_4-GCE were much larger than that at the bare GCE. It is doubtless that the increased redox peak currents should be attributed to the immobilized APTS-Fe_3O_4. It has been reported that Fe_3O_4 nanoparticles and amino-functionalized Fe_3O_4 nanoparticles possess excellent adsorptivity [28, 29]. Therefore, the immobilized APTS-Fe_3O_4 can adsorb more aminopyrine molecules on the electrode surface to increase the redox peak current. Moreover, the oxidation peak potential obtained at APTS-Fe_3O_4-GCE was 0.386 V, and the reduction peak potential was 0.256 V. The ΔE_p was 0.13 V, which was lower than that obtained at the bare GCE. This phenomenon can be explained as the catalytic activity of APTS-Fe_3O_4 [30]. From the above investigation, it is clear that APTS-Fe_3O_4-GCE showed high sensitivity for aminopyrine determination. Based on this, APTS-Fe_3O_4-GCE was selected as the working electrode. Since the oxidation peak response is much higher than the corresponding reduction peak, the oxidation peak current of aminopyrine was used in the following experiments.

Optimization of determination parameters

The effect of buffer pH on the electrochemical responses of 0.2 mM aminopyrine on APTS-Fe_3O_4-GCE was investigated in 0.1 M PBS by cyclic voltammetry. From Fig. 4, it can be seen that the oxidation peak current increased with increasing pH from 3.0 to 12.0, which might be attributed to that the aminopyrine can be easily oxidized at basic condition. Considering the possible interference in strong basic solution,

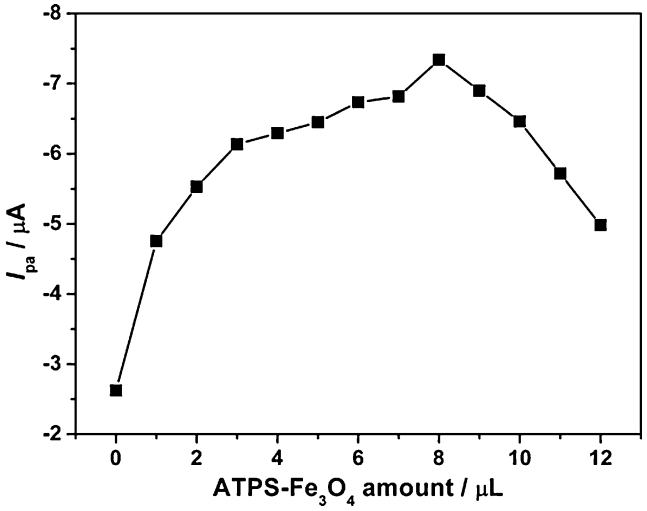

Fig. 4 Effect of APTS-Fe_3O_4 volume on the oxidation current response of aminopyrine

pH 9.0 was chosen. Moreover, the oxidation peak potential of aminopyrine shifted negatively when the solution pH increased from 5.0 to 12.0. A linear regression equation was obtained as $E_{pa}(v) = -0.011pH + 0.4786$ ($R = 0.9977$). According to the equation of $-0.011x/n = -0.059$ [7], where n is the electron transfer number and x is the number of hydrogen ion participating in the reaction, so x/n=5.36, indicating that the electrochemical oxidation of aminopyrine should be a complicated electrode process.

The amount of APTS-Fe_3O_4 on the GCE surface directly influenced the electrode thickness, further influenced the determination sensitivity. Therefore, the relationship between the oxidation peak current of aminopyrine and the immobilized volume of 3 mg/mL APTS-Fe_3O_4 dispersion was investigated in 0.1 M PBS (pH 9.0) by differential pulse voltammetry. As shown in Fig. 5, the oxidation peak current increased gradually when improving the volume of the APTS-Fe_3O_4 dispersion from 0 to 8 μL. Further increasing the volume of APTS-Fe_3O_4 dispersion, the oxidation peak current conversely decreased. Considering the determination sensitivity, 8 μL was chosen as the optimum immobilization amount.

The effect of accumulation potential and accumulation time on the oxidation peak current of aminopyrine was also investigated. In Fig. 6A, it is clear that the oxidation peak current increased with accumulation time up to 200 s at a fixed accumulation potential of −0.20 V. Afterwards, the peak current increased much slightly as further extending accumulation time. This phenomenon could be attributed to the saturated adsorption of aminopyrine at the electrode surface. Considering both determination sensitivity and work efficiency, the optimal accumulation time of 200 s was employed. As can be seen in Fig. 6B, with the accumulation potential shifting from 0.40 to −0.20 V at a fixed accumulation time of 200 s, the oxidation peak

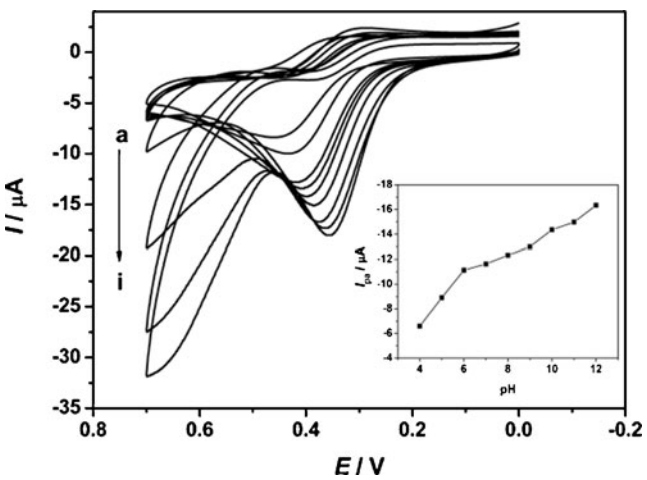

Fig. 5 Influence of solution pH on the cyclic voltammetric response of aminopyrine at the scan rate of 100 mV/s. a–i 4.0, 5.0, 6.0, 7.0, 8.0, 9.0, 10.0, 11.0, 12.0

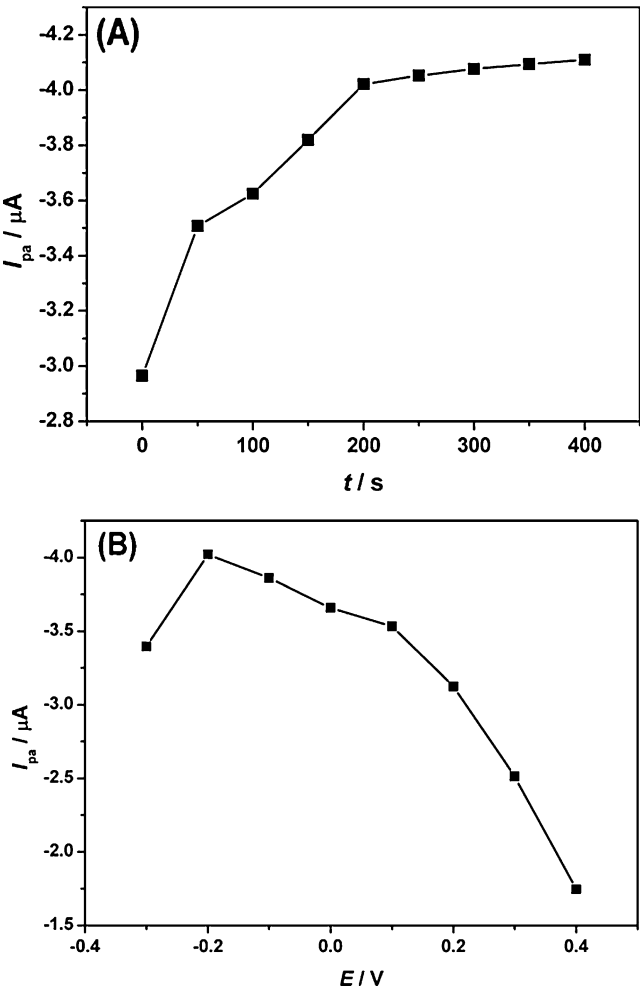

Fig. 6 Effect of accumulation time (**A**) and accumulation potential (**B**) on the oxidation current response of 0.1 mM aminopyrine in 0.1 M pH 9.0 PBS

current increased remarkably. Then, the decrease of oxidation peak current was observed with further decreasing accumulation potential. The maximum oxidation peak current was obtained at −0.20 V, which was used as optimal accumulation potential.

Chronocoulometry

The electrochemically effective areas of the bare GCE and APTS-Fe_3O_4-GCE were investigated by chronocoulometry using 0.1 mM $K_3Fe(CN)_6$ as a model compound in 1 M KCl solution, and the results were shown in Fig. 7. According to the equation given by Anson [31], $Q = 2nFAD^{1/2}Ct^{1/2}/\pi^{1/2} + Q_{dl} + Q_{ads}$, where n is electron transfer number, A is the electrochemically effective area of the working electrode, D is the diffusion coefficient of $K_3Fe(CN)_6$, C is the concentration of $K_3Fe(CN)_6$, Q_{dl} is the double-layer charge and Q_{ads} is the Faradaic charge due to the oxidation of $K_3Fe(CN)_6$, other symbols have their usual meanings. The electrochemically effective area can be obtained from the intercept of the Anson's plots (Q versus $t^{1/2}$) when the values of n, F, D, and C are known. It has been reported that the value of D of 0.1 mM $K_3Fe(CN)_6$ in 1 M KCl is 7.6×10^{-6} cm^2 s^{-1} [32]. In this work, the slopes of Anson's plots for GCE and APTS-Fe_3O_4-GCE are 3.383 and 6.608 μC/$s^{1/2}$, respectively. Therefore, A was calculated to be 0.05599 cm^2 for the bare GCE and 0.1094 cm^2 for APTS-Fe_3O_4-GCE. It is clear that the electrode surface area increased remarkably after modification, which can increase the electrode reaction site, enhance the oxidation response of aminopyrine, and improve the determination sensitivity. Moreover, the large electrode surface can also adsorb more aminopyrine molecules on the electrode surface to increase the current response. For proving it, chronocoulometry was investigated in 0.1 M PBS (pH 9.0) containing 0.2 mM aminopyrine. From the intercepts of the Anson's plots (Q versus $t^{1/2}$), the charge (Q_{ads}) corresponding to the adsorbed component (after background charge correction from the backward step) can be obtained, and the results showed that Q_{ads} of aminopyrine at the bare GCE and APTS-Fe_3O_4-GCE were 2.159 and 13.39 μC, respectively. Obviously, the value of Q_{ads} of aminopyrine at the APTS-Fe_3O_4-GCE increased significantly in comparison with that at the bare GCE, indicating that APTS-Fe_3O_4 can offer more effective accumulation of aminopyrine.

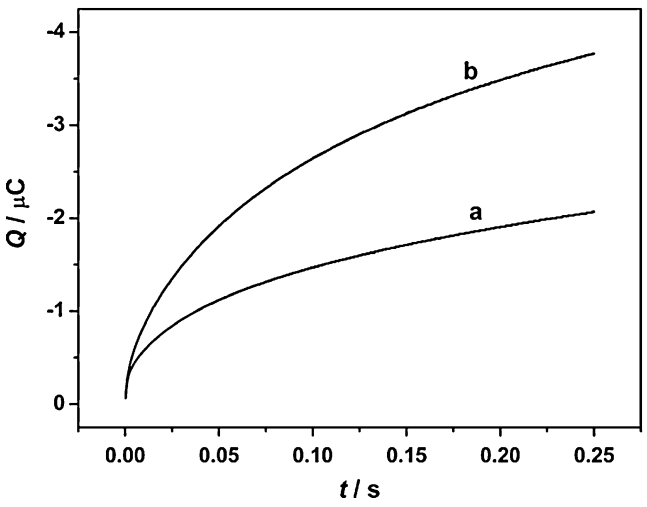

Fig. 7 Chronocoulometry curves of GCE (*a*) and APTS-Fe_3O_4-GCE (*b*) in 0.1 mM $K_3Fe(CN)_6$ containing 1 M KCl

Calibration curve

Differential pulse voltammetry was carried out for the determination of aminopyrine due to its high sensitivity. As can be seen in Fig. 8, the oxidation peak current increased linearly with aminopyrine concentration in the range of 0.5–100 and 100–1,600 μM. The corresponding regression equation can be expressed as $I_{pa} = -0.05957c - 0.091$ (μA, μM, $R = 0.9969$) and $I_{pa} = -0.01423c - 3.5142$ (μA, μM, $R = 0.9956$). The limit of detection (LOD) was 0.1 μM (S/N=3). The analytical performances of the fabricated electrode for aminopyrine determination were compared with other methods, and the results were listed in Table 1. It can be seen that APTS-Fe_3O_4-GCE showed wide linear range and relative low LOD. Though LC–MS–MS showed lower detection limits than the proposed method in this paper, it requires sophisticated and expensive instrumentation with large size, complicated operation, skilled operator, high cost, and long detection time. However, the proposed method in this work showed a significant improvement with cheap instrument, simple electrode preparation, low cost, and short detection time. Six APTS-Fe_3O_4-GCE were prepared by the same

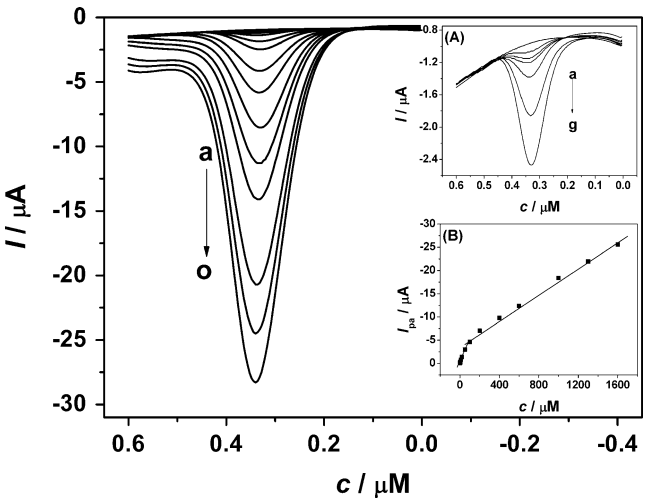

Fig. 8 (A) Differential pulse voltammograms of different concentrations of aminopyrine in pH 9.0 PBS (from a to o: 0, 0.5, 1, 2, 4, 10, 20, 50, 100, 200, 400, 600, 1,000, 1,300, 1,600 μM). (B) Calibration curve

Table 1 The aminopyrine determination performance of the proposed method compared with other methods

Methods	Linear range (μM)	LOD (μM)	Refs.
HPLC-ED	57.3–8,600	4.3	[6]
RPC-AD	0.432–432	0.3	[5]
CE-ED	50–100,000	0.12	[3]
LC–MS–MS	0.00345–34.5	0.00345	[1]
APTS-Fe_3O_4-GCE	0.5–1,600	0.1	This work

procedure independently, and the relative standard deviation (RSD) value for the determination of 5.0 μM aminopyrine was calculated as 3.78%, which indicated the modified electrode had good repeatability.

Effect of interferents

Caffeine, phenacetin, antipyrine, and barbital are the main coexisting substance in compound tablet and injecta samples, so the electrochemical responses of aminopyrine in the presence of the above four compounds at the APTS-Fe_3O_4-GCE were studied. From the differential pulse voltammograms, the oxidation peak potentials were located at 0.796, 1.124, and 1.34 V for phenacetin, antipyrine, and caffeine, respectively. Barbital showed no electrochemical signal at APTS-Fe_3O_4-GCE in the potential range from 0 to 1.4 V. These oxidation peak potentials were all higher than that of aminopyrine (0.33 V). The oxidation peak potential separations were 0.466, 0.794, and 1.01 V for aminopyrine and phenacetin, aminopyrine and antipyrine, and aminopyrine and caffeine, respectively. These separations were large enough for aminopyrine determinations in the mixed solution. Furthermore, some inorganic ions were also investigated. It is found that 500-fold concentrations of Na^+, K^+, NH_4^+, Ca^{2+}, Mg^{2+}, Fe^{3+}, ,Al^{3+}, Mn^{2+}, Zn^{2+}, Ni^{2+}, Cu^{2+}, Pb^{2+}, F^-, Cl^-, SCN^-, SO_4^{2-}, CO_3^{2-}, and NO_3^- do not interfere with the oxidation signal of 10 μM aminopyrine (peak current change <5%). These results indicated that the method investigated in this work possessed excellent selectivity.

Practical application

The proposed method was applied to detect aminopyrine content in the tablets and injecta. The determination results were listed in Table 2. It is clear that the determination results are in good agreement with the manufacturers' stated contents of aminopyrine in the tablets and injecta. For further confirming the practical applicability, the standard addition method was employed. The analytical results were also shown in Table 2. It can be seen that aminopyrine concentrations in the samples could be satisfactory detected with the recovery in the range from 99.7% to 102%, indicating the potential application of the proposed electrode.

Conclusions

In this work, APTS-Fe_3O_4-GCE was used to determine aminopyrine. Compared with the bare GCE, the oxidation peak current of aminopyrine obtained at APTS-Fe_3O_4-GCE increased significantly and the corresponding oxidation peak potential decreased obviously, indicating that APTS-Fe_3O_4 can effectively catalyze the oxidation of aminopyrine. Under the optimum experimental conditions, the oxidation peak current was proportional to aminopyrine concentration in the range from 0.5 to 100 and 100 to 1,600 μM with the detection limit of 0.1 μM. The presence of coexisting substances, such as caffeine, phenacetin, antipyrine, and barbital, showed no interferences to the determinations. The proposed method was further successfully applied to tablet and injecta samples containing aminopyrine, which demonstrated a new method for aminopyrine determination. The investigated method showed good analytical performance with lower detection limit, higher sensitivity, and selectivity.

Table 2 Determination of aminopyrine in pharmaceutical formulations using APTS-Fe_3O_4-GCE

Sample	Stated content	Determined content	Added (μM)	Found (μM)	RSD (%)	Recovery (%)
Aminopyrine and caffeine tablet	0.15 [a]	0.145 [a]	10	0.998	3.21	99.8
Compound amantadine hydrochloride tablet	0.15 [a]	0.148 [a]	10	0.998	2.18	99.8
Compound aminopyrine phenacetin and caffeine tablet	0.1 [a]	0.103 [a]	10	0.997	2.57	99.7
Compound aminophenzone injection	0.0715 [b]	0.0702 [b]	10	0.102	3.64	102
Compound aminopyrine and antipyrine injection	0.05 [b]	0.053 [b]	10	0.999	1.88	99.9

[a] The unit is grams per tablet

[b] The unit is grams per milliliter

Acknowledgements The authors thank the National Natural Science Foundation of China (No.21075078) and the Natural Science Foundation of Shandong province of China (No. ZR2010BM005) for the financial supports.

References

1. Lin D, Zhang Y, Wang X, Zhang Z, Zhu J, Ye F, Ye Y (2010) Chromatographia 71:927–931
2. Brodie B, Axelrod J (1950) J Pharmacol Exp Ther 99:171–184
3. Zhou W, Liu J, Wang E (1995) J Chromatogr A 715:355–360
4. Shimada K, Nagase Y (1980) J Chromatogr B 181:51–57
5. Li H, Wang E (1995) Electroanalysis 7:280–282
6. Wang E, Zhou J (1990) Microchem J 42:259–266
7. Sun W, Yang M, Li Y, Jiang Q, Liu S, Jiao K (2008) J Pharm Biomed Anal 48:1326–1331
8. Wang C, Shao X, Liu Q, Qu Q, Yang G, Hu X (2006) J Pharm Biomed Anal 42:237–244
9. Abbaspour A, Mirzajani R (2007) J Pharm Biomed Anal 44:41–48
10. Zhang W, Xu B, Hong Y, Yu Y, Ye J, Zhang J (2010) J Solid State Electrochem 14:1713–1718
11. Baby TT, Aravind SSJ, Arockiadoss T, Rakhi RB, Ramaprabhu S (2010) Sensor Actuat B 145:71–77
12. Bonk SM, Lisdat F (2009) Biosens Bioelectron 25:739–744
13. Burgoa Calvo ME, Domínguez Renedo O, Arcos Martínez MJ (2007) Talanta 74:59–64
14. Mazloum-Ardakani M, Rajabi H, Mirjalili B, Beitollahi H, Akbari A (2010) J Solid State Electrochem 14:2285–2292
15. Fang B, Zhang C, Zhang W, Wang G (2009) Electrochim Acta 55:178–182
16. Sun W, Wang D, Li G, Zhai Z, Zhao R, Jiao K (2008) Electrochim Acta 53:8217–8221
17. Cheng Y, Liu Y, Huang J, Li K, Xian Y, Zhang W, Jin L (2009) Electrochim Acta 54:2588–2594
18. He Q, Gan T, Zheng D, Hu S (2010) J Solid State Electrochem 14:1057–1064
19. Yin H, Zhou Y, Ai S, Chen Q, Zhu X, Liu X, Zhu L (2010) J Hazard Mater 174:236–243
20. Yin H, Zhou Y, Ai S, Liu X, Zhu L, Lu L (2010) Microchim Acta 169:87–92
21. El Mhammedi MA, Achak M, Chtaini A (2009) J Hazard Mater 161:55–61
22. Qiu J, Xiong M, Liang R, Peng H, Liu F (2009) Biosens Bioelectron 24:2649–2653
23. Wang S, Tan Y, Zhao D, Liu G (2008) Biosens Bioelectron 23:1781–1787
24. Fan H, Pan Z, Gu H (2010) Microchim Acta 168:239–244
25. Chen C, Liu Y, Gu H (2010) Microchim Acta 171:371–376
26. Xu Q, Bian X, Li L, Hu X, Sun M, Chen D, Wang Y (2008) Electrochem Commun 10:995–999
27. Ma M, Zhang Y, Yu W, Shen H, Zhang H, Gu N (2003) Colloids Surf A 212:219–226
28. Wang J, Zheng S, Shao Y, Liu J, Xu Z, Zhu D (2010) J Colloid Interface Sci 349:293–299
29. Iram M, Guo C, Guan Y, Ishfaq A, Liu H (2010) J Hazard Mater 181:1039–1050
30. Zhang S, Zhao X, Niu H, Shi Y, Cai Y, Jiang G (2009) J Hazard Mater 167:560–566
31. Anson F (1964) Anal Chem 36:932–934
32. Adams R (1969) Electrochemistry at solid electrodes. Marcel Dekker, New York